

# Pseudogap phase and fractionalization : an experimental test

Anurag Banerjee,<sup>1</sup> Alvaro Ferraz,<sup>2</sup> and Catherine Pépin<sup>1</sup>

<sup>1</sup>*Institut de Physique Théorique, Université Paris-Saclay, CEA, CNRS, F-91191 Gif-sur-Yvette, France.*

<sup>2</sup>*International Institute of Physics - UFRN, Natal, Brazil.*

The pseudogap (PG) regime of the underdoped cuprates arguably remains one of the most enigmatic phenomena of correlated quantum matter. Recent theoretical ideas suggest that “fractionalized” bosonic fields can lead to the PG phase, by opening a gap in the anti-nodal (AN) region of the Brillouin zone. Such fractionalized boson can originate from modulated particle-particle pairs or pair density wave (PDW), a magnetic stripe, or a modulated spin one particle-hole pair like a spin density wave (SDW) boson, among others. The main picture goes as follows. Electrons under strong coupling tend to form different types of unstable bosons at high temperatures. As the temperature goes down, the compact object gets extremely unstable, and to minimize the entropy, it finally fractionalizes into elementary components, linked by a constraint. The process of fractionalization involves, in this way, an emergent gauge field directly linked to the constraint. This, in turn, couples to the Fermi surface of electronic carriers and opens a gap in the AN region, which is partly responsible for the PG phase. Alternative theoretical approaches invoke a simple coexistence between the multiple quasi-degenerate orders like charge density wave (CDW), superconductivity (SC), and magnetic orders at low temperatures. This scenario attributes the PG formation as a “vestigial” order showing up at  $T^*$ , which acts as a precursor to the zero temperature orders. This intricate situation calls for a key experimental test, enabling us to discriminate between the various theoretical scenarios. In this paper, we focus on the case where the PDW boson has fractionalized into a CDW and SC order below  $T^*$ , and we compare this to the situation where the two orders simply coexist.

## I. THEORETICAL CONCEPTS FOR “FRACTIONALIZED” PDW AND COEXISTING ORDERS

We focus on the idea of a PDW order parameter, fractionalizing into a CDW and SC orders. This choice has the advantage of simplicity since these two orders are ubiquitously observed<sup>1-6</sup> inside the PG region. The CDW is given by  $\hat{\chi} = g_\chi \sum_{\mathbf{k},\sigma} c_{\mathbf{k},\sigma}^\dagger c_{\mathbf{k}+\mathbf{Q}_0,\sigma}$  with  $\mathbf{Q}_0$  being the modulation wave vector, and  $g_\chi$  the interaction responsible for forming CDW pairs. Similarly, the SC order is defined as  $\hat{\Delta} = g_\Delta \sum_{\mathbf{k},\sigma} \sigma c_{\mathbf{k},\sigma} c_{-\mathbf{k},-\sigma}$ , where  $c^\dagger$  ( $c$ ) are the standard creation (annihilation) operators for electrons and  $g_\Delta$  is the interaction forming the Cooper pairs (the conjugated operators are straightforward). The origin of such unstable boson at high temperature most certainly comes from the strong coupling regime of the electrons<sup>7-9</sup> but this is not the main focus of the paper. The PDW is defined as  $\hat{\Delta}_{\text{PDW}} = g_{\text{PDW}} \sum_{\mathbf{k},\sigma} \sigma c_{\mathbf{k},\sigma} c_{-(\mathbf{k}+\mathbf{Q}_0),-\sigma}$ . It turns out that it can be written as a combination of elementary operators, i.e.,  $\hat{\Delta}_{\text{PDW}} = \frac{g_{\text{PDW}}}{2g_\Delta g_\chi} [\hat{\Delta}, \hat{\chi}^*]$  and  $\hat{\Delta}_{\text{PDW}}^* = \frac{g_{\text{PDW}}}{2g_\Delta g_\chi} [\hat{\chi}, \hat{\Delta}^*]$  where  $[a, b]$  stands for the commutator of the operators  $a$  and  $b$ .

### A. Fractionalization

The key idea leading to the fractionalization of the PDW is that at the PG temperature  $T^*$  a  $U(1)$  gauge field emerges

$$\begin{aligned} \hat{\Delta}_r &\rightarrow \hat{\Delta}_r e^{i\theta_r}, \\ \hat{\chi}_r &\rightarrow \hat{\chi}_r e^{i\theta_r}, \end{aligned} \quad (1)$$

under which  $\hat{\Delta}_{\text{PDW}}$  and  $\hat{\Delta}_{\text{PDW}}^*$  remain invariant. Fluctuations of the gauge field in an effective field theory generates

a constraint (note that the  $\Delta$  and  $\chi$  have the dimension of energy)

$$|\Delta_r|^2 + |\chi_r|^2 = (E^*)^2, \quad (2)$$

where  $E^*$  is an energy scale typical of the PG, which is constant in temperature, and with respect to spatial variations, but doping dependent. When coupling to the conduction electrons is considered, the constraint of Eq.(2) opens a gap, primarily in the AN region of the Fermi surface, leading to the presence of Fermi arcs in the nodal region.<sup>10-13</sup>

The typical effective field theory describing the  $\hat{\Delta}_{\text{PDW}}$ -mode, has the form of a quantum rotor model

$$S = \frac{1}{2} \int d^2x \sum_{a,b=1}^2 |\omega_{ab}|^2, \quad \text{with } \omega_{ab} = z_a \partial_\mu z_b - z_b \partial_\mu z_a, \quad (3)$$

with  $z_1 = \Delta/E^*$ ,  $z_2 = \chi/E^*$ ,  $z_1^* = \Delta^*/E^*$ ,  $z_2^* = \chi^*/E^*$ . The gauge fluctuations within the transformation  $z_a \rightarrow z_a e^{i\theta}$ , ( $z_a^* \rightarrow z_a^* e^{-i\theta}$ ) is naturally described by the constraint  $\sum_a |z_a|^2 = Cst$ , which is equivalent to Eq.(2).

### B. Coexistence

By contrast in the model of coexisting phase the action takes the form of a standard  $\varphi^4$ -field theory

$$\begin{aligned} S = \frac{1}{2} \int d^2x \sum_{a=1}^2 & \left( |\partial_\mu z_a|^2 + \mu_a |z_a|^2 \right) \\ & + \sum_{a,b=1}^2 g_{ab} |z_a|^2 |z_b|^2. \end{aligned} \quad (4)$$

In Eq.(4) the two modes are in coexistence and interact with each other, but there is no form of chirality and no emerging gauge field as in Eq. (3).

### C. Phase diagram

We compare the phase diagram of cuprate superconductors within the two scenarios mentioned above for the PG.<sup>14-16</sup> However, note that the reality is undoubtedly more complicated due to the proximity to the Mott transition. Nevertheless, restricting these two sets of ideas simplify the following discussion enormously.

In the coexistence scenario, a precursor of the SC or CDW orders forms at  $T^*$ . Most of the theories that have been advanced consider PDW as a precursor at  $T^*$ . Since a PDW order is notoriously tricky to stabilize compared to homogeneous SC, a certain amount of fluctuations is present below  $T^*$  making the PDW phase fluctuating. At a lower temperature  $T_{co}$ , two-dimensional charge modulations do form.<sup>17-21</sup> Part of the corresponding spectral weight is forming a genuinely three-dimensional order under an applied magnetic field.<sup>22-24</sup> But at zero fields, the phase of the 2D CDW is fluctuating with coupling to the lattice, which produces a very inhomogeneous response  $\chi \cos(\mathbf{Q}_0 \cdot \mathbf{r} + \theta_r)$  with  $\theta_r$  strongly varying from site to site.<sup>25-29</sup> At an even lower temperature SC order forms at  $T_c$ , leading us to identify the freezing of the SC phase  $\Delta \exp(i\theta_{EM})$ , with the electromagnetic field  $\partial_\mu \theta_{EM}$  being expelled from the sample.

In contrast, in the fractionalized PDW scenario,<sup>10-13</sup> the PDW order fails to form at  $T^*$ . However, the gauge field emerges, leading to the constraint of Eq. (2). Note that fractionalized PDW does not exhaust the system's total spectral weight but might coexist with fermions and uniform PP pairs, and modulated PH pairs. At  $T_{co}$  charge modulations emerge, and similar to the coexistence scenario, the phase of the modulations fluctuates from site to site. The difference between the two scenario sets up below  $T_c$ , where the SC order sets up. Now we have  $\Delta \exp(i(\theta + \theta_{EM}))$ .  $\partial_\mu \theta_{EM}$  is set to zero by the Meissner effect due to the presence of non fractionalized SC pairs. Consequently, the whole phase of superfluid density is set to be constant, with  $\partial_\mu \theta = 0$ . This affects the phase of the CDW, which becomes insensitive to the impurities and the coupling to the lattice. This effect has been reported recently,<sup>30-33</sup> with an intriguing observation of uniform CDW phase inside vortices under the application of the magnetic field. Here we consider another consequence of fractionalized PDW: namely, its effects on the current in the Josephson junction setup.

## II. THE MODEL EXPERIMENTAL SET-UP

We propose the experimental setup pictured in Fig. (1). A Josephson junction (JJ) is considered, with underdoped cuprates compounds in two terminals A and B separated by an insulating material. Below  $T^*$ , the terminals in A and B

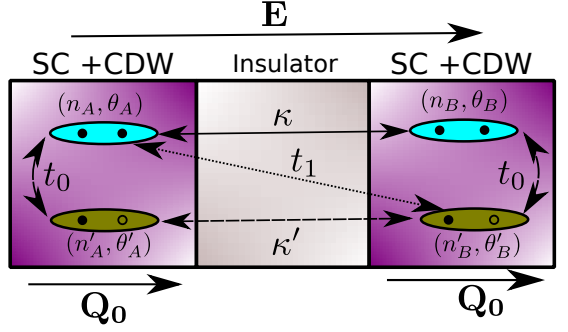


FIG. 1. Josephson junction setup when the applied electric field is parallel to the charge density wave modulation wavevector  $\mathbf{Q}_0$ . The different possible hoppings between the pairs are presented schematically.  $\kappa$  denotes a PP-pair hopping from terminal A to B, and vice versa.  $\kappa'$  represents the same for the hopping of PH-pairs across the junction. The inter-junction conversion of PP-pair to a PH-pair is denoted by  $t_1$  and the same within the junction by  $t_0$ .

access the PG regime and we expect these terminals to display both SC and CDW orders at low temperatures. The JJ is oriented such that the modulation wave vector is parallel to the junction. Moreover, in the present situation, an electric field  $\mathbf{E}$  is applied in the same direction as CDW wavevector  $\mathbf{Q}_0$ .

We consider the following wavefunctions for the A and B subsystems

$$\begin{aligned} |\psi_A\rangle &= \sqrt{n_A}e^{i\theta_A} + \sqrt{n'_A}e^{i\theta'_A}, \\ |\psi_B\rangle &= \sqrt{n_B}e^{i\theta_B} + \sqrt{n'_B}e^{i\theta'_B}, \end{aligned} \quad (5)$$

where  $(n_{A,B}, \theta_{A,B})$  are the superfluid density and phases of SC states on terminals A and B respectively, and  $(n'_{A,B}, \theta'_{A,B})$  are the corresponding CDW density and phases. At a steady state, we take  $\theta'_A = \mathbf{Q}_0 \cdot \mathbf{r}$  and  $\theta'_B = \mathbf{Q}_0 \cdot (\mathbf{r} + \delta)$ . The most generic set of Schrödinger's equations write, with  $\psi = (\sqrt{n_A}e^{i\theta_A}, \sqrt{n_B}e^{i\theta_B}, \sqrt{n'_A}e^{i\theta'_A}, \sqrt{n'_B}e^{i\theta'_B})$

$$i\hbar \frac{\partial}{\partial t} \psi = \begin{pmatrix} \mu_\Delta & \kappa & t_0 & t_1 \\ \kappa & -\mu_\Delta & t_1 & t_0 \\ t_0 & t & V_A & \kappa' \\ t_1 & t_0 & \kappa' & V_B \end{pmatrix} \psi, \quad (6)$$

where  $\kappa$  and  $\kappa'$  are the hopping integrals for particle-particle (PP) and particle-hole (PH) pairs across the junctions. The parameter  $\mu_\Delta = eU$ , where  $U$  is the electrical potential applied to the PP pairs. In terms of the applied electric field  $\mathbf{E}$ , this becomes  $\mu_\Delta = -e\mathbf{E}r_{A,B}$ , where  $r_{A,B}$  is the distance with respect to the center. However, in this study,  $\mu_\Delta$  is assumed to be a constant as in the standard JJ setup.<sup>34</sup> The parameter  $t_1$  represents the tunneling between the PP pairs in the junction A (resp. B) to the modulated PH pairs in junction B (resp. A), whereas  $t_0$  is the same type of tunneling within a junction. The electric field acts on the CDW sector<sup>35</sup> as  $V_{A,B} = eE\bar{\rho}\theta'_{A,B}$ , where  $\bar{\rho} = n'/Q_0$  is an effective CDW density divided by the ordering wave vector  $\mathbf{Q}_0$ .

We have assumed that the superfluid density and the CDW densities are constant throughout the JJ. Although this is not necessary; such assumption simplifies the following analysis enormously. The Eqs.(6) can be decoupled into (For details see Appendix (A))

$$\frac{\partial \bar{n}}{\partial t} = \frac{4}{\hbar} \left[ -\kappa n \sin \theta + \sqrt{nn'} \cos \frac{\phi}{2} \times \left( t_0 \sin \frac{\theta' - \theta}{2} - t_1 \sin \frac{\theta' + \theta}{2} \right) \right], \quad (7)$$

$$\frac{\partial \theta}{\partial t} = \frac{2}{\hbar} \left[ \mu_\Delta + \sqrt{\frac{n'}{n}} \sin \frac{\phi}{2} \times \left( t_0 \sin \frac{\theta - \theta'}{2} - t_1 \sin \frac{\theta + \theta'}{2} \right) \right], \quad (8)$$

$$\frac{\partial \bar{n}'}{\partial t} = \frac{4}{\hbar} \left[ -\kappa' n' \sin \theta' + \sqrt{nn'} \cos \frac{\phi}{2} \times \left( t_0 \sin \frac{\theta' - \theta}{2} - t_1 \sin \frac{\theta' + \theta}{2} \right) \right], \quad (9)$$

$$\frac{\partial \theta'}{\partial t} = \frac{1}{\hbar} \left[ (V_A - V_B) - 2\sqrt{\frac{n'}{n}} \sin \frac{\phi}{2} \times \left( t_0 \sin \frac{\theta' - \theta}{2} - t_1 \sin \frac{\theta' + \theta}{2} \right) \right], \quad (10)$$

$$\frac{\partial \phi}{\partial t} = -\frac{1}{\hbar} \left[ (V_A + V_B) + 2\kappa \cos \theta + 2\kappa' \cos \theta' - \frac{2\delta n}{\sqrt{nn'}} \left( t_0 \cos \frac{\theta - \theta'}{2} + t_1 \cos \frac{\theta + \theta'}{2} \right) \right], \quad (11)$$

with  $\theta = \theta_B - \theta_A$ ,  $\theta' = \theta'_B - \theta'_A$ ,  $\phi = \theta'_B + \theta'_A - \theta_A - \theta_B$ ,  $\bar{n} = n_B - n_A$ ,  $\bar{n}' = n'_A - n'_B$ ,  $\delta n = n' - n$ . Furthermore, we assumed that the density of PP-pairs and PH-pairs in both the terminal are similar, i.e.  $n \simeq n_A \simeq n_B$ ,  $n' \simeq n'_A \simeq n'_B$ . The variation of  $\phi$  can be simplified further in the limit where  $n \simeq n'$ ,  $\delta n \ll n$ . In this limit, the Eq. (11) simplifies to,

$$\frac{\partial \phi}{\partial t} \approx -\frac{1}{\hbar} \left[ (V_A + V_B) + 2\kappa \cos \theta + 2\kappa' \cos \theta' \right]. \quad (12)$$

Next we elucidate on the other parameters. The difference of the electric field on the CDW sector can be simplified to  $V_A - V_B = -(eE n'/Q_0) \theta' \equiv -r_0 \theta'$ , where we have introduced a new parameter  $r_0 = eE n'/Q_0$ . Similarly, the average potential acting on the CDW sector due to the applied electric field can be treated as constant for simplicity, i.e.  $V_A + V_B = \eta$ .

### III. JOSEPHSON EFFECT

#### A. Coexistence case : Josephson effect

When the two orders coexist at  $T \leq T_c$ , the phase of the CDW fluctuates from site to site, and we can safely ignore the hopping from a PP-pair to a PH-pair, as the quantum entanglement between the orders is weak. Therefore, we put the parameters  $t_0 = \langle \psi_{SC}^{A(B)} | \psi_{CDW}^{A(B)} \rangle = 0$  and

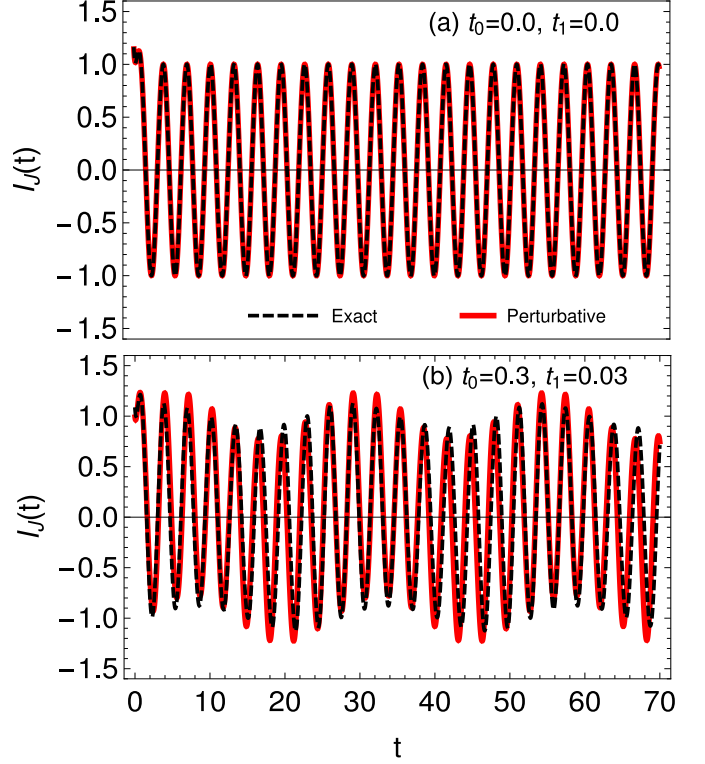


FIG. 2. The variation of Josephson current with time for the setup presented in Fig. (1), i.e., the applied electric field is parallel to the charge modulation wavevector. Here we compare the exact numerical results with the analytical form of the current calculated perturbatively. (a) Shows the situation when the two orders coexist, for a vanishing  $t_0$  and  $t_1$ . In this situation, the perturbative calculations are exact. The initial transient current regime for CDW order vanishes at a long-time limit, and we are left with the simple ac-Josephson effect. (b) Presents the Josephson current for the situation when the entanglement between the orders forms a fractionalized PDW or PDW with a finite  $t_0 = 0.3$ ,  $t_1 = 0.03$ . The perturbative calculations and the numerical analysis shows a good match. Interestingly, the presence of entanglement between CDW and SC orders induces a beat-like modulation of the Josephson current, which can be contrasted with the simple coexistence scenario presented above.

$t_1 = \langle \psi_{SC}^{A(B)} | \psi_{CDW}^{B(A)} \rangle = 0$  in Eq.(6). Still, the Josephson current is modified due to the presence of the CDW,<sup>34,36</sup> with

$$I_J = -\frac{1}{2} \frac{\partial \bar{n}}{\partial t} - \frac{1}{\pi} \frac{\partial \theta'}{\partial t}. \quad (13)$$

Note that the two fluids couple in the opposite way to the field – the tunneling of the charge two bosons contributes to the conventional SC Josephson current. In contrast, the variation of the phase creates a charge imbalance in the case of the CDW and generates an additional current. However, since the parameters  $t_0$  and  $t_1$  vanishes, the Eqns. (7-12) simplifies enormously. Solving for Eq.(13) we get

$$I_J = \frac{2\kappa n}{\hbar} \sin \left( \frac{2\mu_\Delta}{\hbar} t + C_1 \right) + \frac{C_2 r_0}{\pi \hbar} e^{-r_0 t}. \quad (14)$$

Here  $C_1$  and  $C_2$  are constants of integration and depends on the initial experimental setup. The first term in Eq.(14) is the standard Josephson current, whereas the second term is characteristic of the CDW in the situation of coexisting order. Since the SC and CDW orders are disconnected, we only observe a transient response from the CDW phase variation. We have plotted the current  $I_J$  as a function of time  $t$  in Fig. (2a) for the coexistence of CDW and SC. The parameters used to obtain Fig. (2a) are given by  $\mu_\Delta = 1.0$ ,  $n = 1.0$ ,  $n' = 1.0$ ,  $r_0 = 3.0$ ,  $\eta = 0.3$ ,  $\kappa = 0.5$ ,  $\kappa' = 0.6$  with  $t_1 = t_0 = 0$ . We have also used the initial conditions,  $\theta(t = 0) = 0$ ,  $\phi(0) = 0$ , and  $\theta'(0) = 0.6$ . Initially at  $t = 0$ , the transient CDW regime quickly paves the way to a standard form of the Josephson current for an SC. In this situation,  $I_J(t)$  from the exact numerical calculations presented in black dotted trace and the analytical form of Eq. (14) depicted in red thick trace in Fig. (2a) matches exactly.

### B. Fractionalized PDW case : Josephson effect

We begin by noting that for a fractionalized PDW case the CDW phase  $\theta'$  is such that

$$\begin{aligned}\theta'_A &= \mathbf{Q}_0 \cdot \mathbf{x} + \delta\theta'_A, \\ \theta'_B &= \mathbf{Q}_0 \cdot (\mathbf{x} + \delta) + \delta\theta'_B,\end{aligned}\quad (15)$$

where  $\delta$  is a dephasing from electrode A to B. In the setup of Fig. (1),  $\delta$  is the distance between the two electrodes. Whereas in Fig. (5a), the dephasing is the phase-shift of the CDW wavevector in the direction perpendicular to the electrodes. The main difference between the coexisting case is that now  $\theta$  and  $\theta'$  are not independent. Since the phase of  $\Delta_{PDW}$  is coupled to the EM field but has  $\mathbf{Q}_0$  modulations as well, we have

$$\theta = \delta\theta' + \theta_{EM}, \quad (16)$$

where  $\theta_{EM}$  is the electromagnetic phase. Assuming that we are deep inside the SC phase, with un-fractionalized Cooper pairs around, the Meissner effect leads to  $\partial_\mu\theta_{EM} = 0$ , or in other words, to a uniform EM field. From Eq.(16) the phase  $\theta$  coming from the fractionalized PDW is also uniform, leading to  $\partial_\mu\delta\theta' = 0$ . Hence a uniform CDW is induced inside the SC phase, an astonishing result that has been reported in Scanning Tunneling Microscopy (STM) experiment.<sup>30</sup> Since all the phases are fixed, we now get a finite tunneling  $t_1$  and  $t_0$  back and forth from the modulated CDW and SC phases, and Eqs. (7-12) needs to be solved with  $t, t_0 \neq 0$ . We have obtained the Josephson current perturbatively in Appendix (B). The Josephson current in the first order perturbative calcula-

tions is given by

$$\begin{aligned}I_J &= \frac{2\kappa n}{\hbar} \sin\left(\frac{2\mu_\Delta}{\hbar}t + C_1\right) + \frac{C_2 r_0}{\pi\hbar} e^{-r_0 t} \\ &\quad - \frac{2\sqrt{nn'}}{\hbar} \cos\frac{\phi_0}{2} \left(t_0 \sin\frac{\theta'_0 - \theta_0}{2} - t_1 \sin\frac{\theta'_0 + \theta_0}{2}\right) \\ &\quad + \frac{2}{\pi\hbar} \sqrt{\frac{n'}{n}} \sin\frac{\phi_0}{2} \left(t_0 \sin\frac{\theta_0 - \theta'_0}{2} - t_1 \sin\frac{\theta_0 + \theta'_0}{2}\right).\end{aligned}\quad (17)$$

The time evolution of zeroth order( $t_0 = 0, t_1 = 0$ ) solutions of  $\theta_0$ ,  $\theta'_0$ , and  $\phi_0$  is given by

$$\theta_0 = \frac{2\mu_\Delta}{\hbar}t + C_1, \quad (18)$$

$$\theta'_0 = \frac{C_2}{\hbar} e^{-r_0 t}, \quad (19)$$

$$\phi_0 = -\frac{\eta}{\hbar}t + C_3 + \frac{2\kappa'}{r_0\hbar} \text{Ci}[C_2 e^{-r_0 t}] - \frac{\kappa}{\mu_\Delta} \sin\left(\frac{2\mu_\Delta}{\hbar}t + C_1\right), \quad (20)$$

where again  $C_3$  is a constant of integration and  $\text{Ci}[x]$  is the cosine integral function.

We have displayed the current of Eq. (17) in Fig. (2b) for the same set of parameters as in Fig. (2a) albeit with a finite  $t_0 = 0.3, t_1 = 0.03$ . The perturbative analytical calculations matches well with the exact numerical form of the current. The Josephson current for the fractionalized PDW displays a beat-like structure which is strikingly distinguishable from the coexistence case. This provides us with the first experimental prediction – If the PG phase of the underdoped cuprates supports a PDW or fractionalized PDW state, the ac-Josephson current should develop a beat-like form as shown in Fig. (2b). Whereas if the orders simply coexist in the PG phase the ac-Josephson current in long-times will follow the conventional form.

#### 1. Frequencies and envelope of the AC Josephson current

The Josephson current for a fractionalized PDW state shows a beat-like structure that suggests multiple frequencies contribute to the AC Josephson current. To get the frequency, we need to perform a Fourier transform of the AC Josephson current to the frequency domain.

We simplify the Eq. (17) by assuming that the inter junction PP to PH hopping amplitude is small compared to the intra-junction hoppings, i.e.,  $t_1 \ll t_0$ . In an experimental scenario, this requires using a barrier to decay the PH hoppings across the junction. However, for a finite but small  $t_1$ , will not create any qualitative difference to the discussion below. Also, in a long time limit, the transient current regime from the CDW vanishes, i.e.,  $\theta'_0 \rightarrow 0$ . Following the manipulations detailed

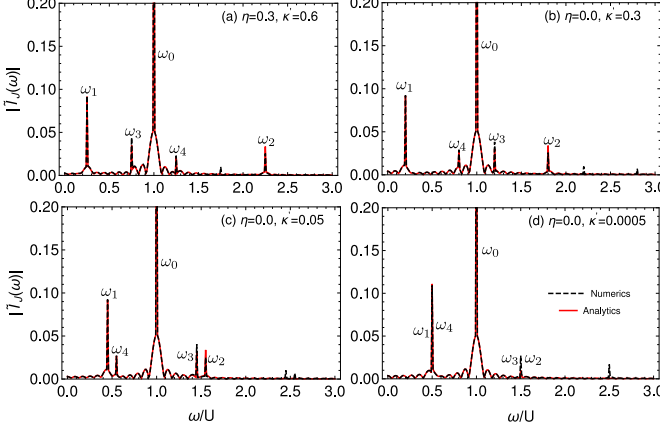


FIG. 3. Exhibits the primary  $\omega_0$  and additional frequencies  $\omega_i$  of AC Josephson current for  $t_0 = 0.3, t_1 = 0.0$ . Here  $\kappa$  and  $\eta$  are material-dependent parameters. As the potential difference between the two terminals dominates the material-dependent parameters, the number of peaks reduces due to the merging of peaks as shown in (c-d). The additional peaks for  $U \gg \eta + 2\kappa'$  are at the half-odd integer multiples of the primary peak  $\omega_0$ .

in Appendix. (C), we obtain

$$I_J \approx \frac{t_0 \sqrt{nn'}}{\hbar} [\mathcal{J}_0(b) \{ \sin a_+ t + \sin a_- t \} + \mathcal{J}_1(b) \{ \sin ((a_+ + \xi)t) - \sin ((a_- + \xi)t) + \sin a_- t - \sin a_+ t \} + \frac{2\kappa n}{\hbar} \sin \xi t], \quad (21)$$

where  $\mathcal{J}_\nu(x)$  is the Bessel function of first kind of the  $\nu$ -th order. Also we have redefined

$$a_\pm = \frac{1}{2} \left( \frac{2\mu_\Delta}{\hbar} \pm \frac{\eta}{\hbar} \pm \frac{2\kappa'}{\hbar} \right), \quad (22)$$

$$b = \frac{\kappa}{2\mu_\Delta}, \quad (23)$$

$$\xi = \frac{2\mu_\Delta}{\hbar}. \quad (24)$$

Since, all the terms are directly proportional to  $t$ , one can easily read off the frequencies for the AC current, by performing a Fourier transform. This is given by

$$\tilde{I}_J(\omega) = \frac{\kappa n}{\hbar} \delta(\omega - \xi) + \frac{t_0 \sqrt{nn'}}{2\hbar} [(\mathcal{J}_0(b) + \mathcal{J}_1(b)) \delta(\omega - a_-) + \mathcal{J}_1(b) \delta(\omega - a_+ - \xi) - \mathcal{J}_1(b) \delta(\omega - a_- - \xi) + (\mathcal{J}_0(b) - \mathcal{J}_1(b)) \delta(\omega - a_-)]. \quad (25)$$

The primary frequency  $\xi$  is the usual AC-Josephson frequency. The other frequencies are the additional originating due to the entanglement of the two orders. The ratio of the primary to the few additional frequency is given by,

$$\frac{\omega_1}{\omega_0} = \frac{1}{2} - \left( \frac{\eta + 2\kappa'}{4eU} \right), \quad (26)$$

$$\frac{\omega_4}{\omega_0} = \frac{1}{2} + \left( \frac{\eta + 2\kappa'}{4eU} \right), \quad (27)$$

$$\frac{\omega_2}{\omega_0} = \frac{3}{2} + \left( \frac{\eta + 2\kappa'}{4eU} \right), \quad (28)$$

$$\frac{\omega_3}{\omega_0} = \frac{3}{2} - \left( \frac{\eta + 2\kappa'}{4eU} \right), \quad (29)$$

where  $\omega_{i-1}$  are the  $i$ -th delta-function peak of Eq. (25) and used the fact that  $\mu_\Delta = eU$ , where  $U$  is the DC potential applied across the terminals. It is clear that for the large potential difference between the two junctions, i.e.,  $U \gg \eta + 2\kappa'$ , the second term of all the ratios vanishes. Moreover, the ratio between the primary and additional frequencies will occur at half-odd integers, i.e.,  $1/2, 3/2, 5/2, \dots$ . However, the peak strength will diminish for the higher-order term as the Bessel functions of higher-order determines the strength of the additional peaks.

We have presented in Fig. (3) the Fourier transform of the Josephson current given in Eq. (17) numerically in black dashed lines and compared with the Eq. (25) in red. The dominant peaks of the AC Josephson junction are well captured in our approximate analysis. The primary peak  $\omega_0$  arising from the normal AC Josephson effect remains unchanged for all the parameters. In Fig. (3a) and Fig. (3b) when  $U \sim \eta + 2\kappa'$ , the four additional peaks are well separated and well-resolved. As the parameters is chosen such that  $U \gg \eta + 2\kappa'$ , the two peaks merge with each other as shown in Fig. (3c) and Fig. (3d). This leads to an apparent reduction in the number of peaks. Interestingly, at a high potential difference between the terminals, the additional frequencies are at the half-odd integers of  $\omega_0$ , as expected from our analysis. Studying such frequency dependence of the AC Josephson current peaks will give strong evidence for the fractionalized PDW state.

We have also obtained the envelope for the oscillation observed for the fractionalized PDW situation. The details for obtaining the same is presented in Appendix (D). To do this we performed a few simplifications. First, we assume that the inter junction PP to PH hopping amplitude is small compared to the intra-junction hoppings, i.e.  $t_1 \ll t_0$ . This is not necessary a priori but it simplifies the following discussion. Experimentally, this requires hindering the  $t_1$  hopping by using a suitable barrier. Secondly, since the envelope exists even in the long-time limit the transient response can be safely ignored. Thirdly, the expressions of current is first order perturbative in  $t_0$  hence  $t_0 \ll \kappa$ . We find that the expression for the current in this limit becomes,

$$I_J \approx \frac{n}{\hbar} \left[ \sqrt{\kappa^2 + t_0^2 + 2\kappa t_0 \cos \chi_1} + \sqrt{\kappa^2 + t_0^2 + 2\kappa t_0 \cos \chi_2} \right] \sin(\theta_0). \quad (30)$$

where  $\chi_1 = (\phi_0 - \theta_0)/2$  and  $\chi_2 = (\phi_0 + \theta_0)/2$ .

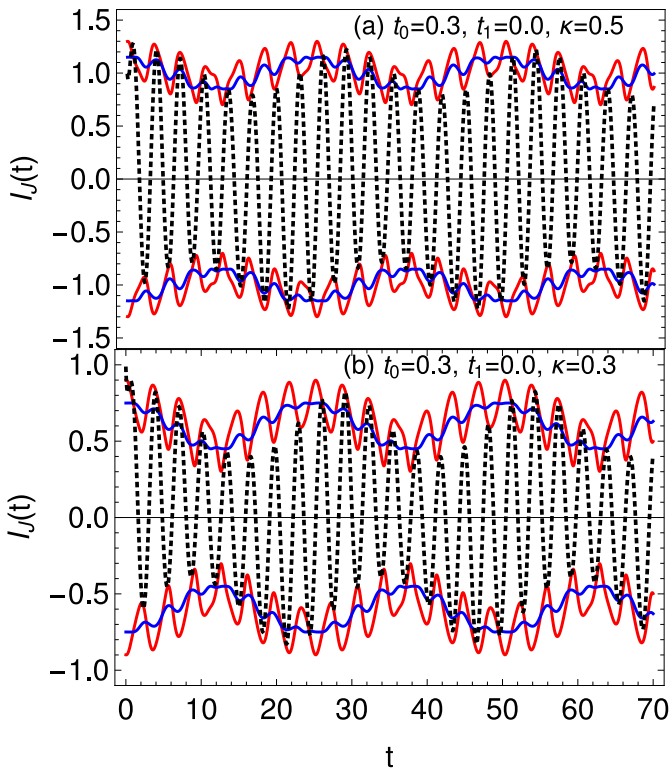


FIG. 4. Presents the evolution of the beat-like form of the Josephson current for two different parameters (a)  $\kappa = 0.5$ , (b)  $\kappa = 0.3$ . The total envelope for the oscillation is governed by the red traces. The blue trace shows the slower oscillation of the envelope which is controlled by the first term of Eq. (30) and hence by  $\chi_1 = (\phi_0 - \theta_0)/2$

The total envelope shown by the red trace in Fig. (4a) and Fig. (4b) is controlled by the both  $\chi_1$  and  $\chi_2$ , and in particular the term inside the square bracket in Eq. (30). However, the slower oscillation shown by the blue traces in Fig. (4) is controlled by the  $\chi_1$  term. We also obtained another insight into the nature of the beat-like Josephson current. The beat-like oscillations for JJ with fractionalized PDW becomes better resolved as the inter junction PP-hopping  $\kappa$  becomes comparable to the conversion rate of intra-junction PP-pairs to PH pairs  $t_0$ . Experimental observation of such dependence will also signal the fractionalized PDW in the pseudogapped phase of the underdoped cuprates.

## 2. Modulation wavevector of the fractionalized PDW

It is also possible to detect the PDW modulation wavevector by varying the dephasing parameter  $\delta$  between the two electrodes and by investigating its effect on the Josephson current. First, to see this, we study the Josephson current at  $t = 0$  with the given width of the junction,  $\delta$ . At  $t = 0$  we have from Eq. (15),  $\theta' = Q_0\delta$  and  $\phi = Q_0\delta + \gamma$ , where  $\gamma$  can be set to a constant. Similarly,  $\theta = C_1$  is also a constant at  $t = 0$ , which depends on the initial condition of the JJ setup. The expression for this current for the coexistence of orders is given

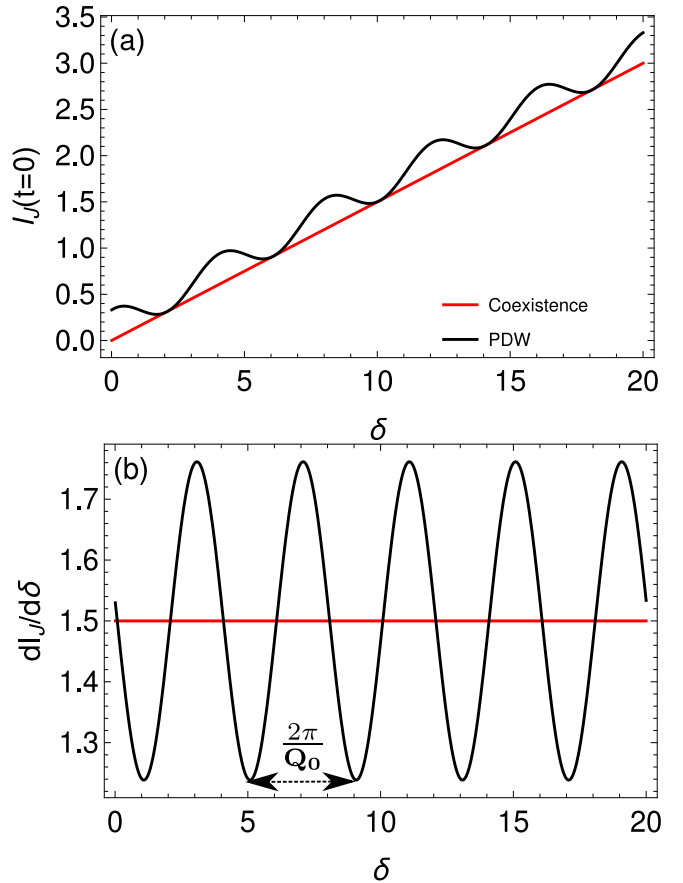


FIG. 5. (a) Depicts the variation of Josephson current at  $t = 0$  with the width of the insulating region,  $\delta$ . For a simple coexistence of two orders, the current shows a linear increase with the increasing slope, with the slope proportional to the CDW modulation wavevector. However, for PDW or a fractionalized PDW state, the Josephson current reveals a modulation with  $\delta$ . (b) Shows the derivative of the data presented in the (a). The PDW modulation wavevector  $Q_0$  controls the oscillation of the Josephson current with  $\delta$ .

by

$$I_J(t = 0) = \frac{2\kappa n}{\hbar} \sin C_1 + \frac{r_0}{\pi \hbar} Q_0 \delta. \quad (31)$$

Clearly, the expression is linearly increasing with the width of the junction. This is presented in Fig. (5a) in the red trace for  $r_0 = 0.3$ ,  $\kappa n = 1.0$ ,  $C_1 = \pi$  and  $Q_0 = \pi/2$ . Similarly, the expression for the current for the fractionalized PDW at  $t = 0$  becomes

$$\begin{aligned} I_J(t = 0) = & \frac{2\kappa n}{\hbar} \sin C_1 + \frac{r_0}{\pi \hbar} Q_0 \delta \\ & - \frac{2\sqrt{nn'}}{\hbar} \cos \frac{Q_0 \delta + \gamma}{2} \left( t_0 \sin \frac{Q_0 \delta - C_1}{2} - t_1 \sin \frac{Q_0 \delta + C_1}{2} \right) \\ & + \frac{2}{\pi \hbar} \sqrt{\frac{n'}{n}} \sin \frac{Q_0 \delta + \gamma}{2} \left( t_0 \sin \frac{C_1 - Q_0 \delta}{2} - t_1 \sin \frac{C_1 + Q_0 \delta}{2} \right). \end{aligned} \quad (32)$$

In this situation, along with the linear increase of the current with  $\delta$ , there is also an oscillation proportional to  $Q_0 \delta$ . We

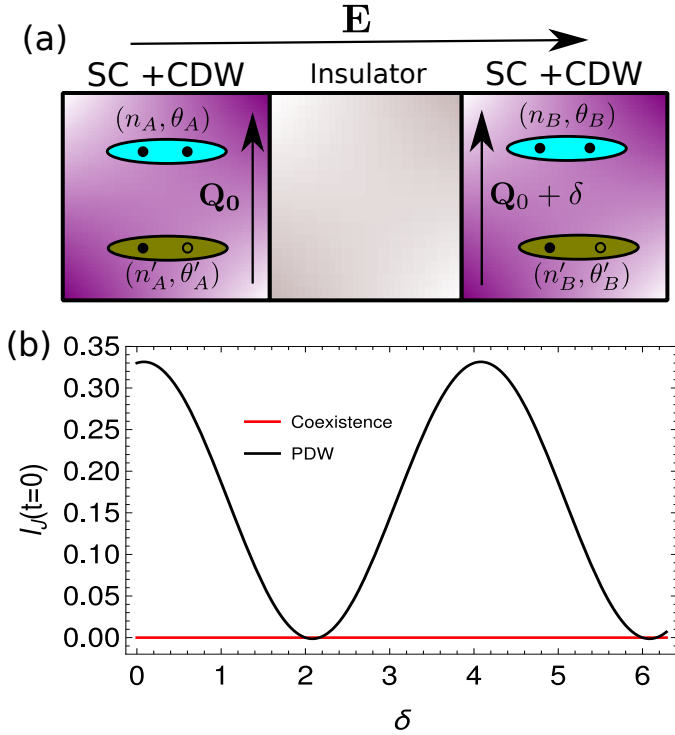


FIG. 6. (a) Shows a Josephson junction setup in which the electric field is perpendicular to the charge modulation wavevector. The CDW modulations in the two terminals are dephased by a factor of  $\delta$  here. (b) Depicts the evolution of the Josephson current with the dephasing parameter  $\delta$  at  $t = 0$ . For a simple coexistence of orders, the current at  $t = 0$  with the dephasing parameter vanishes. However, for the fractionalized PDW the Josephson current again modulates with the modulation proportional to the CDW wavevector  $Q_0$ .

have plotted the same in Fig. (5b) in black trace for the same parameter as (a) with  $t_0 = 0.3$ ,  $t_1 = 0.03$  and  $\gamma = 0$ . The modulation wavevector can be clearly identified if we take the derivative of  $I_J(0)$  w.r.t. to  $\delta$ . We depicted the same in Fig. (5b) and it clearly shows periodic oscillations with the wavelength,  $2\pi/Q_0$ . Therefore, it also becomes an essential tool in experiments to determine the magnitude of the PDW wavevector. Note in the experiments this JJ setup requires measuring the Josephson current as soon as the external electric field is switched on. In Appendix (E 1), we discuss the difficulty of detecting such signals at long times after the electric field is switched on.

Fig. (6a) shows a different JJ setup where the modulation wavevector is perpendicular to the electric field. Here  $\delta$  denotes the phase-shift of the CDW wavevector in the B electrode wrt the A. In this situation,  $V_A$  and  $V_B$  vanishes and hence  $r_0 = \eta = 0$ . The Josephson current at  $t = 0$  in this scenario for both cases is given by Eq. (E1) with a vanishing second term. In Fig. (6b) we plot the Josephson current obtained at  $t = 0$ . The fractionalized PDW case again displays a modulation controlled by  $2\pi/Q_0$ . In Appendix (E 2), we explore the possibility of detecting the signal at a time  $t$  after the electric field is turned on, in this setup.

#### IV. INVERSE JOSEPHSON EFFECT

##### A. Coexistence case : inverse Josephson effect

In the previous section, we used a constant DC-voltage  $U$  across the junction, leading to an AC-Josephson current. It is also possible to apply a microwave AC-voltage to the junction, such that,  $U(t) = U + \tilde{U} \cos \omega t$ . Here  $U$  is the constant DC-Voltage. Note that we have used an insulating barrier, so the normal current passing through the junction will vanish. Solving for the Josephson current, for the simple coexistence of orders, the Josephson current is given by

$$I_J = \frac{2\kappa n}{\hbar} \sum_{m=-\infty}^{\infty} \left[ (-1)^m \sin \left( C_1 + \frac{2eU}{\hbar} t - m\omega t \right) \times \mathcal{J}_m \left( \frac{2e\tilde{U}}{\hbar\omega} \right) \right] + \frac{C_2 r_0}{\pi\hbar} e^{-r_0 t}, \quad (33)$$

where  $m$  is an integer and  $\mathcal{J}_m$  is the Bessel function of the first kind of order  $m$ . The time average of this quantity gives the DC current  $I_{DC}$ . The long time average of the oscillatory term vanishes unless the frequency  $\omega$  is some integral multiple of the applied DC-Voltage  $U$  in the units where  $(2e)/\hbar = 1$ . The transient current also fades away in the long time limit. The DC-current in that scenario is given by,

$$|I_{DC}| \approx \frac{2\kappa n}{\hbar} \sum_{m=-\infty}^{\infty} \delta_{m\omega, U} (-1)^m \mathcal{J}_m \left( \frac{\tilde{U}}{\omega} \right) \sin C_1 \quad (34)$$

which leads to sharp  $\delta$  peaks at the integer multiples of the AC-frequency  $\omega$ . These peaks are known as Shapiro spikes.

We have solved Eqns. (7-12) for an AC-voltage of the form  $U(t) = U + \tilde{U} \cos \omega t$  and plotted the DC current as a function of the  $U$  in the units of  $(2e)/\hbar = 1$  in Fig. (7). In all these figures we have used the parameters same as in Fig. (2) with AC-frequency  $\omega = 1$  and amplitude  $\tilde{U} = 1.2$ ,  $C_1 = \pi/2$ . For the coexistence of orders  $t_0, t_1 = 0$  and we find in Fig. (7a) the expected sharp Shapiro spikes at the integer multiple of  $\omega$ .

##### B. Fractionalized PDW : inverse Josephson effect

Next, we solve the Eqns. (7-12) numerically for an AC-voltage of the same form but a finite  $t_0, t_1$  and track the evolution of the Shapiro spikes. In Fig. (7b) we present the results for  $t_0 = 0.01, t_1 = 0.001$ , i.e., a small entanglement between the two orders leading to a weak PDW state. We see that multiple weak peaks emerge as soon as the entanglement between the two orders is turned on. Such extra peaks get stronger as the overlap between the charge, and SC order becomes large in Fig. (7c). Finally, for a strong fractionalized PDW state, the Shapiro spikes appear at different DC-voltage than the integer multiple of  $\omega$ . Therefore, our calculations suggest that additional DC-current peaks in the inverse Josephson junction setup will strongly favor fractionalized PDW scenario. However, for a competing order scenario, the Shapiro spikes will remain robust.

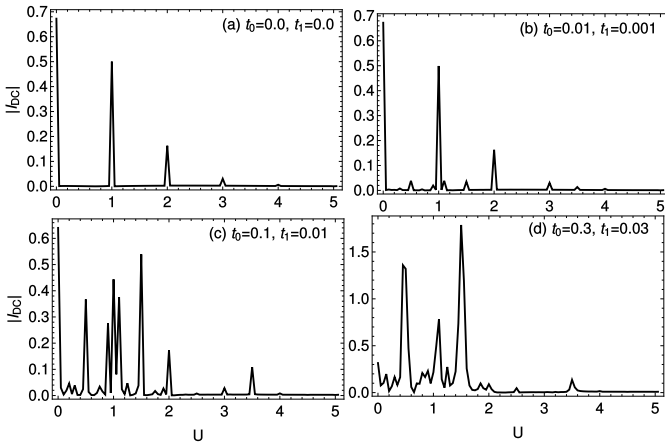


FIG. 7. Demonstrates the total DC-current with the applied DC voltage  $U$  across the junctions in the inverse Josephson setup. In (a) we set  $t_0 = 0, t_1 = 0$  the parameter corresponding to the simple coexistence of CDW and SC orders. The sharp Shapiro spikes can be observed when the applied DC-voltage  $U$  is equal to the integer multiple of the terahertz frequency  $\omega$ . In (b)-(d) we plot the same for finite  $t_0, t_1$  which corresponds to the fractionalized PDW scenario. In (b)  $t_0, t_1$  is small, and other peaks start developing in between the two Shapiro spikes. In (c)-(d) These additional peaks become stronger as the entanglement between the two orders is increased.

## V. DISCUSSION

One of the most unusual features of the cuprates is the proliferation of quasi-degenerate orders in the underdoped regime, near the mysterious pseudogap phase. These orders include experimentally established orders, like the SC state, CDW order, and antiferromagnetic state, but it may also include putative “hidden” orders like the PDW, for which experimental evidence is still lacking. Conceptually, it is natural to advocate that a very unusual interplay of states is responsible for the formation of the PG.<sup>37</sup> Many routes are proposed to drive forward this set of ideas.

Firstly there is the proposal of a vestigial order.<sup>38-42</sup> In this framework, the system tends to form all the potentially degenerate orders. These orders compete with each other within a standard Ginzburg-Landau description, resulting in some precursor order which can account for the development of the pseudogap state. For example, we could see the competition between the SC state and CDW state with a precursor or mother state formed by a long-ranged PDW order.<sup>32,33,43</sup>

A more unconventional proposal affirms that such appearance of quasi-degenerate states can lead to an emergent symmetry.<sup>44-49</sup> Concretely, considering only the SC and CDW orders for simplicity, the corresponding emergent symmetry is the SU(2) group, rotating between the two states. However, the emergent symmetry is fragile and gets easily destroyed by a small tuning of appropriate parameters. Nevertheless, the idea of emergent symmetry is the first illustration of some entangled states, in this particular case between SC and CDW, which is arguably the characteristic of cuprates. Indeed some proposals have suggested that around optimal doping, cuprate

superconductors form a maximally entangled state, a fixed point with a strong coupling that can be described within the holographic framework.

Somewhere in-between the ideas of ultimately entangled fixed point and vestigial order remains another original proposal.<sup>10-13</sup> In this approach, at  $T^*$  the system is ripe to form all possible particle-particle and particle-hole pairs that symmetry allows. This includes particle-particle pairs with zero and finite momentum, particle-hole pairs with finite momentum, some of which are magnetically inert and others active. At lower temperatures, under pressure to order, some pairs become unstable and fractionalize into more robust pairs. A gauge field emerges and a corresponding constraint generated by the fluctuations lead to the opening of a gap and, thus, to the pseudogap phase itself.

This paper proposes an experiment that can distinguish between two direct orders in competition and with other fractionalized state. We focused on the case of a fractionalized PDW particle-particle pair which can turn into SC and CDW pairs. Our findings are that in the case of fractionalized PDW phase:

- we observe a beat-like structure of AC-Josephson current when a constant DC-Voltage is applied across the junction
- the additional frequencies for the AC Josephson current are at the half-odd integer multiple of the normal Josephson frequency for a large value of constant DC voltage.
- we can detect modulations of the Josephson current at  $t = 0$  by varying the width of the junction with a period proportional to the CDW wavevector  $\mathbf{Q}_0$ .
- in the inverse Josephson setup, the induced DC-current have additional peaks other than the standard Shapiro spikes.

Any experiments that can test these features will be instrumental in differentiating between the different scenarios of the pseudogap phase.

## VI. ACKNOWLEDGEMENT

The authors thank Maxence Grandadam, J.C. Séamus Davis, and Yvan Sidis for valuable discussions. This work has received financial support from the ERC, under grant agreement AdG694651-CHAMPAGNE.

## Appendix A: The Schrödinger equations

In this section we provide complimentary details on how to derive Eq.(6). We rewrite Eq.(6) as

$$i\hbar \frac{\partial}{\partial t} (\sqrt{n_A} e^{i\theta_A}) = \mu_\Delta \sqrt{n_A} e^{i\theta_A} + \kappa \sqrt{n_B} e^{i\theta_B} + t_0 \sqrt{n'_A} e^{i\theta'_A} + t_1 \sqrt{n'_A} e^{i\theta'_B}, \quad (\text{A1})$$

$$i\hbar \frac{\partial}{\partial t} (\sqrt{n_B} e^{i\theta_B}) = -\mu_\Delta \sqrt{n_B} e^{i\theta_B} + \kappa \sqrt{n_A} e^{i\theta_A} + t_0 \sqrt{n'_B} e^{i\theta'_B} + t_1 \sqrt{n'_A} e^{i\theta'_A}, \quad (\text{A2})$$

$$i\hbar \frac{\partial}{\partial t} \left( \sqrt{n'_A} e^{i\theta'_A} \right) = V_A \sqrt{n'_A} e^{i\theta'_A} + \kappa' \sqrt{n'_B} e^{i\theta'_B} + t_0 \sqrt{n_A} e^{i\theta_A} + t_1 \sqrt{n_B} e^{i\theta_B}, \quad (\text{A3})$$

$$i\hbar \frac{\partial}{\partial t} \left( \sqrt{n'_B} e^{i\theta'_B} \right) = V_B \sqrt{n'_B} e^{i\theta'_B} + \kappa' \sqrt{n'_A} e^{i\theta'_A} + t_0 \sqrt{n_B} e^{i\theta_B} + t_1 \sqrt{n_A} e^{i\theta_A}. \quad (\text{A4})$$

Expanding Eq.(A1) and taking the complex conjugate of it yields

$$i\hbar \left( \sqrt{\dot{n}_A} + i\dot{\theta}_A \sqrt{n_A} \right) e^{i\theta_A} = \mu_\Delta \sqrt{n_A} e^{i\theta_A} + \kappa \sqrt{n_B} e^{i\theta_B} + t_0 \sqrt{n'_A} e^{i\theta'_A} + t_1 \sqrt{n'_A} e^{i\theta'_B}, \quad (\text{A5})$$

$$-i\hbar \left( \sqrt{\dot{n}_A} - i\dot{\theta}_A \sqrt{n_A} \right) e^{-i\theta_A} = \mu_\Delta \sqrt{n_A} e^{-i\theta_A} + \kappa \sqrt{n_B} e^{-i\theta_B} + t_0 \sqrt{n'_A} e^{-i\theta'_A} + t_1 \sqrt{n'_A} e^{-i\theta'_B}. \quad (\text{A6})$$

Adding Eqs.(A5) and (A6) leads to

$$\frac{\partial n_A}{\partial t} = \frac{2}{\hbar} \left[ \kappa \sqrt{n_A n_B} \sin \theta + t_0 \sqrt{n_A n'_A} \sin(\theta'_A - \theta_A) + t_1 \sqrt{n'_B n_A} \sin(\theta'_B - \theta_A) \right], \quad (\text{A7})$$

where  $\theta = \theta_B - \theta_A$ . Next subtracting Eq. (A5) from Eq. (A6) leads to

$$\frac{\partial \theta_A}{\partial t} = -\frac{1}{\hbar} \left[ \mu_\Delta + \kappa \sqrt{\frac{n_B}{n_A}} \cos \theta + t_0 \sqrt{\frac{n'_A}{n_A}} \cos(\theta'_A - \theta_A) + t_1 \sqrt{\frac{n'_B}{n_A}} \cos(\theta'_B - \theta_A) \right], \quad (\text{A8})$$

Next repeating the same procedure for the Eq. (A2), we obtain

the corresponding equations for  $n_B$  and  $\theta_B$  as follows,

$$\frac{\partial n_B}{\partial t} = \frac{2}{\hbar} \left[ -\kappa \sqrt{n_A n_B} \sin \theta + t_0 \sqrt{n_B n'_B} \sin(\theta'_B - \theta_B) + t_1 \sqrt{n'_A n_B} \sin(\theta'_A - \theta_B) \right], \quad (\text{A9})$$

$$\frac{\partial \theta_B}{\partial t} = \frac{1}{\hbar} \left[ \mu_\Delta - \kappa \sqrt{\frac{n_A}{n_B}} \cos \theta - t_0 \sqrt{\frac{n'_B}{n_B}} \cos(\theta'_B - \theta_B) - t_1 \sqrt{\frac{n'_A}{n_B}} \cos(\theta'_A - \theta_B) \right]. \quad (\text{A10})$$

We define  $\bar{n} = n_B - n_A$ , subtracting Eq. (A7) from Eq. (A9), lead to

$$\begin{aligned} \frac{\partial \bar{n}}{\partial t} = & \frac{2}{\hbar} \left[ -2\kappa \sqrt{n_A n_B} \sin \theta \right. \\ & + t_0 \left( \sqrt{n_B n'_B} \sin(\theta'_B - \theta_B) - \sqrt{n_A n'_A} \sin(\theta'_A - \theta_A) \right) \\ & \left. + t_1 \left( \sqrt{n'_A n_B} \sin(\theta'_A - \theta_B) - \sqrt{n'_B n_A} \sin(\theta'_B - \theta_A) \right) \right]. \end{aligned} \quad (\text{A11})$$

Approximating, that the density of of particle-particle pairs and particle-hole pairs in both the terminals is similar in the steady state, i.e.,  $n_A \approx n_B = n$  and  $n'_A \approx n'_B = n'$  and defining  $\phi = \theta'_B - \theta'_A - \theta_A - \theta_B$ , we obtain

$$\frac{\partial \bar{n}}{\partial t} = \frac{4}{\hbar} \left[ -\kappa n \sin \theta + \sqrt{n n'} \cos \frac{\phi}{2} \times \left( t_0 \sin \frac{\theta' - \theta}{2} - t_1 \sin \frac{\theta' + \theta}{2} \right) \right], \quad (\text{A12})$$

where  $\theta' = \theta'_B - \theta'_A$ . Following the same procedure and approximation we can obtain the differential equation for  $\theta$ , which is given by

$$\begin{aligned} \frac{\partial \theta}{\partial t} = & \frac{2}{\hbar} \left[ \mu_\Delta + \sqrt{\frac{n'}{n}} \sin \frac{\phi}{2} \right. \\ & \left. \times \left( t_0 \sin \frac{\theta - \theta'}{2} - t_1 \sin \frac{\theta + \theta'}{2} \right) \right], \end{aligned} \quad (\text{A13})$$

Repeating the procedure for Eqs. (A3), (A4), we obtain the differential equation for the  $\bar{n}'$  and  $\theta'$ .

$$\begin{aligned} \frac{\partial \bar{n}'}{\partial t} = & \frac{4}{\hbar} \left[ -\kappa' n' \sin \theta' + \sqrt{n n'} \cos \frac{\phi}{2} \right. \\ & \left. \times \left( t_0 \sin \frac{\theta' - \theta}{2} - t_1 \sin \frac{\theta' + \theta}{2} \right) \right], \end{aligned} \quad (\text{A14})$$

$$\begin{aligned} \frac{\partial \theta'}{\partial t} = & \frac{1}{\hbar} \left[ (V_A - V_B) - 2\sqrt{\frac{n'}{n}} \sin \frac{\phi}{2} \right. \\ & \left. \times \left( t_0 \sin \frac{\theta' - \theta}{2} - t_1 \sin \frac{\theta' + \theta}{2} \right) \right], \end{aligned} \quad (\text{A15})$$

Using all these forms for the  $\theta$ 's we can obtain the time evolution equation for the  $\phi$

$$\begin{aligned}\frac{\partial\phi}{\partial t} = & -\frac{1}{\hbar}[(V_A + V_B) + 2\kappa \cos \theta + 2\kappa' \cos \theta' \\ & - \frac{2(n - n')}{\sqrt{nn'}} \left( t_0 \cos \frac{\theta - \theta'}{2} + t_1 \cos \frac{\theta + \theta'}{2} \right)],\end{aligned}\quad (\text{A16})$$

The fourth term on the RHS can be approximately taken to be small when the particle-particle pairs and the particle-hole pairs are of similar strength, i.e.,  $\delta n/n \ll 1$  and thus we obtain

$$\frac{\partial\phi}{\partial t} \approx -\frac{1}{\hbar}[(V_A + V_B) + 2\kappa \cos \theta + 2\kappa' \cos \theta']. \quad (\text{A17})$$

We need to solve the five coupled differential Eqns. (A12), (A13), (A14), (A15), and (A17).

## Appendix B: Evaluation of Josephson current

The Josephson current is obtained by the expression<sup>34,36</sup>

$$I_J = -\frac{1}{2} \frac{\partial \bar{n}}{\partial t} - \frac{1}{\pi} \frac{\partial \theta'}{\partial t}. \quad (\text{B1})$$

To find this, we need a solution to the equations presented in the previous section. Using the forms for the difference of potential between the two terminal due to charge density modulations as  $V_A - V_B = -eE\bar{\rho}\theta' \equiv -r_0\theta'$ , with the average of the same  $V_A + V_B = \eta$  set to constant. The coupled differential equations can be written in a condensed form as,

$$\frac{\partial \bar{n}}{\partial t} = \frac{4}{\hbar} \left[ -\kappa n \sin \theta + \sqrt{nn'} \cos \frac{\phi}{2} f(t_0, t_1, \theta, \theta') \right], \quad (\text{B2})$$

$$\frac{\partial \theta}{\partial t} = \frac{2}{\hbar} \left[ \mu_\Delta + \sqrt{\frac{n'}{n}} \sin \frac{\phi}{2} f(t_0, t_1, \theta, \theta') \right], \quad (\text{B3})$$

$$\frac{\partial \bar{n}'}{\partial t} = \frac{4}{\hbar} \left[ -\kappa' n' \sin \theta' + \sqrt{nn'} \cos \frac{\phi}{2} g(t_0, t_1, \theta, \theta') \right], \quad (\text{B4})$$

$$\frac{\partial \theta'}{\partial t} = \frac{1}{\hbar} \left[ -r_0 \theta' - 2 \sqrt{\frac{n'}{n}} \sin \frac{\phi}{2} g(t_0, t_1, \theta, \theta') \right], \quad (\text{B5})$$

$$\frac{\partial \phi}{\partial t} = -\frac{1}{\hbar} [\eta + 2\kappa \cos \theta + 2\kappa' \cos \theta']. \quad (\text{B6})$$

Here we have defined,

$$f(t_0, t_1, \theta, \theta') = \left( t_0 \sin \frac{\theta' - \theta}{2} - t_1 \sin \frac{\theta' + \theta}{2} \right), \quad (\text{B7})$$

$$g(t_0, t_1, \theta, \theta') = \left( t_0 \sin \frac{\theta - \theta'}{2} - t_1 \sin \frac{\theta + \theta'}{2} \right). \quad (\text{B8})$$

These equations can be solved using numerical means for any parameter, and Josephson current can be evaluated using Eq. (B1). However, here we discuss an approach to calculate

when the  $t_0$  and  $t_1$  are small parameters that can be incorporated perturbatively in the expression. In this approach, we expand the solutions

$$\bar{n} = \bar{n}_0 + (t_0 + t_1)\bar{n}_1 + (t_0 + t_1)^2\bar{n}_2 + \dots \quad (\text{B9})$$

$$\theta' = \theta'_0 + (t_0 + t_1)\theta'_1 + (t_0 + t_1)^2\theta'_2 + \dots \quad (\text{B10})$$

and so on for other variables, and the subscript represents the perturbative order of the solution. The zeroth-order solution is readily obtained by putting  $t_0 = 0$  and  $t_1 = 0$  in Eq. (B2) to Eq. (B6). The relevant equations becomes,

$$\frac{\partial \bar{n}_0}{\partial t} = -\frac{4\kappa n}{\hbar} \sin \theta_0, \quad (\text{B11})$$

$$\frac{\partial \theta_0}{\partial t} = \frac{2\mu_\Delta}{\hbar}, \quad (\text{B12})$$

$$\frac{\partial \theta'_0}{\partial t} = -\frac{r_0}{\hbar} \theta'_0, \quad (\text{B13})$$

$$\frac{\partial \phi_0}{\partial t} = -\frac{1}{\hbar} [\eta + 2\kappa \cos \theta_0 + 2\kappa' \cos \theta'_0]. \quad (\text{B14})$$

The solution for these equations are readily obtained and these are given by,

$$\theta_0 = \frac{2\mu_\Delta}{\hbar} t + C_1, \quad (\text{B15})$$

$$\theta'_0 = \frac{C_2}{\hbar} e^{-r_0 t}, \quad (\text{B16})$$

and the zeroth order Josephson current becomes,

$$I_J^{(0)} = \frac{2\kappa n}{\hbar} \sin \left( \frac{2\mu_\Delta}{\hbar} t + C_1 \right) + \frac{C_2 r_0}{\pi \hbar} e^{-r_0 t}, \quad (\text{B17})$$

where  $C_1$  and  $C_2$  are the constants of integration. Notice that the first term is the usual Josephson current for a superconducting junction, whereas the second term is a transient current due to the presence of charge orders. When the entanglement between the orders are small, i.e. for a simple coexistence of order Eq. (B17) gives the exact form of the current.

Next we focus on obtaining the first order correction to this current. To this end, we need the zeroth order expression for  $\phi_0$ , which can be obtained by using  $\theta_0$  and  $\theta'_0$  in Eq. (B14),

$$\phi_0 = -\frac{\eta}{\hbar} t + C_3 + \frac{2\kappa'}{r_0 \hbar} \text{Ci} [C_2 e^{-r_0 t}] - \frac{\kappa}{\mu_\Delta} \sin \left( \frac{2\mu_\Delta}{\hbar} t + C_1 \right), \quad (\text{B18})$$

where again  $C_3$  is a constant of integration and  $\text{Ci}[x]$  is the cosine integral function. The first order, equations can now be evaluated by taking the derivative of Eq. (B2) and Eq. (B5) with respect to  $t_0$  and  $t_1$  individually and subsequently setting these small parameter to zero. Therefore the first-order correction for the terms relevant for the Josephson current thus becomes

$$\frac{\partial \bar{n}_1}{\partial t} = \frac{4\sqrt{nn'}}{\hbar} \cos \frac{\phi_0}{2} \left( t_0 \sin \frac{\theta'_0 - \theta_0}{2} - t_1 \sin \frac{\theta'_0 + \theta_0}{2} \right), \quad (\text{B19})$$

$$\frac{\partial \theta'_1}{\partial t} = -\frac{2}{\hbar} \sqrt{\frac{n'}{n}} \sin \frac{\phi_0}{2} \left( t_0 \sin \frac{\theta - \theta'_0}{2} - t_1 \sin \frac{\theta + \theta'_0}{2} \right). \quad (\text{B20})$$

Therefore up to the first order the Josephson current is given by,

$$I_J = \frac{2\kappa n}{\hbar} \sin\left(\frac{2\mu_\Delta}{\hbar}t + C_1\right) + \frac{C_2 r_0}{\pi\hbar} e^{-r_0 t} - \frac{2\sqrt{nn'}}{\hbar} \cos\frac{\phi_0}{2} \left(t_0 \sin\frac{\theta'_0 - \theta_0}{2} - t_1 \sin\frac{\theta'_0 + \theta_0}{2}\right) + \frac{2}{\pi\hbar} \sqrt{\frac{n'}{n}} \sin\frac{\phi_0}{2} \left(t_0 \sin\frac{\theta_0 - \theta'_0}{2} - t_1 \sin\frac{\theta_0 + \theta'_0}{2}\right), \quad (\text{B21})$$

where we can use the time evolution of  $\theta_0$ ,  $\theta'_0$ , and  $\phi_0$  from Eq. (B15), Eq. (B16) and Eq. (B18) respectively. In the main text, this form is compared favorably with the exact current evaluated by solving the equations numerically.

### Appendix C: Extracting the frequencies of the AC Josephson current

The Josephson current for a fractionalized PDW state shows a beat like structure. This suggests multiple frequencies are contributing to the AC Josephson current. This section provides the details to obtain the Josephson current frequencies. To do so, we need to perform a Fourier transform of the AC Josephson current to the frequency domain.

We simplify the Eq. (B21) by assuming that the inter junction PP to PH hopping amplitude is small compared to the intra-junction hoppings, i.e.,  $t_1 \ll t_0$ . In an experimental scenario, this requires using a barrier to decay the PH hoppings across the junction. However, for a finite but small  $t_1$ , will not create any qualitative difference to the discussion below. Also, in a long time limit, the transient current regime from the CDW vanishes, i.e.,  $\theta'_0 \rightarrow 0$ . Hence the current reduces to

$$I_J \approx \frac{2\kappa n}{\hbar} \sin \theta_0 + \frac{2t_0 \sqrt{nn'}}{\hbar} \cos \frac{\phi_0}{2} \sin \frac{\theta_0}{2} - \frac{2t_0}{\pi\hbar} \sqrt{\frac{n'}{n}} \sin \frac{\phi_0}{2} \sin \frac{\theta_0}{2}, \quad (\text{C1})$$

Furthermore, since the  $n \approx n'$  and  $n \sim \mathcal{O}(1)$ , the second term dominates over the third. The expression for the current further simplifies to

$$I_J \approx \frac{2\kappa n}{\hbar} \sin \theta_0 + \frac{2t_0 \sqrt{nn'}}{\hbar} \cos \frac{\phi_0}{2} \sin \frac{\theta_0}{2}. \quad (\text{C2})$$

Using trigonometric identities, the second term becomes,

$$I_2 \approx \frac{t_0 \sqrt{nn'}}{\hbar} \left[ \sin\left(\frac{\theta_0 + \phi_0}{2}\right) + \sin\left(\frac{\theta_0 - \phi_0}{2}\right) \right]. \quad (\text{C3})$$

The  $\theta_0$  and  $\phi_0$  is given by Eq. (B15) and Eq. (B18) respectively. The constant terms do not contribute to the frequency of the AC Josephson frequency, and hence we can ignore them for the following analysis. Next we make a series expansion

for  $Ci[\dots]$  function and neglecting the constant and higher order terms, we obtain

$$I_2 \approx \frac{t_0 \sqrt{nn'}}{\hbar} [\sin(a_+ + b \sin \xi t) + \sin(a_- - b \sin \xi t)], \quad (\text{C4})$$

where we have defined

$$a_\pm = \frac{1}{2} \left( \frac{2\mu_\Delta}{\hbar} \pm \frac{\eta}{\hbar} \pm \frac{2\kappa'}{\hbar} \right) \quad (\text{C5})$$

$$b = \frac{\kappa}{2\mu_\Delta} \quad (\text{C6})$$

$$\xi = \frac{2\mu_\Delta}{\hbar} \quad (\text{C7})$$

Next, we expand

$$\cos(x \sin \theta) = \mathcal{J}_0(x) + 2 \sum_{p=1}^{\infty} \mathcal{J}_{2p}(x) \cos(2p\theta), \quad (\text{C8})$$

$$\sin(x \sin \theta) = 2 \sum_{p=1}^{\infty} \mathcal{J}_{2p+1}(x) \sin((2p+1)\theta), \quad (\text{C9})$$

Where  $\mathcal{J}_\nu(x)$  is the Bessel function of first kind of the  $\nu$ -th order. Neglecting the higher order terms the current in Eq. (C1) becomes

$$I_J \approx \frac{t_0 \sqrt{nn'}}{\hbar} [\mathcal{J}_0(b) \{\sin a_+ t + \sin a_- t\} + \mathcal{J}_1(b) \{\sin((a_+ + \xi)t) - \sin((a_- + \xi)t) + \sin a_- t - \sin a_+ t\}] + \frac{2\kappa n}{\hbar} \sin \xi t \quad (\text{C10})$$

Since, all the terms are directly proportional to  $t$ , one can easily read off the frequencies for the AC current, by performing a fourier transform. This is given by

$$\tilde{I}_J(\omega) = \frac{\kappa n}{\hbar} \delta(\omega - \xi) + \frac{t_0 \sqrt{nn'}}{2\hbar} [(\mathcal{J}_0(b) + \mathcal{J}_1(b))\delta(\omega - a_-) + \mathcal{J}_1(b)\delta(\omega - a_+ - \xi) - \mathcal{J}_1(b)\delta(\omega - a_- - \xi) + (\mathcal{J}_0(b) - \mathcal{J}_1(b))\delta(\omega - a_-)] \quad (\text{C11})$$

The primary frequency  $\xi$  is the usual AC-Josephson frequency. The other frequencies are the additional ones originating due to the entanglement of the two orders. The ratio of the primary to the few additional frequencies is given by,

$$\frac{\omega_1}{\omega_0} = \frac{1}{2} - \left( \frac{\eta + 2\kappa'}{4eU} \right), \quad (\text{C12})$$

$$\frac{\omega_4}{\omega_0} = \frac{1}{2} + \left( \frac{\eta + 2\kappa'}{4eU} \right), \quad (\text{C13})$$

$$\frac{\omega_2}{\omega_0} = \frac{3}{2} + \left( \frac{\eta + 2\kappa'}{4eU} \right), \quad (\text{C14})$$

$$\frac{\omega_3}{\omega_0} = \frac{3}{2} - \left( \frac{\eta + 2\kappa'}{4eU} \right), \quad (\text{C15})$$

$$(\text{C16})$$

where  $\omega_{i-1}$  are the  $i$ -th delta function peak of Eq. (C11). It is clear that for large potential difference between the two junctions i.e.,  $U \gg \eta + 2\kappa'$ , the second term of all the ratios vanish. Moreover, the ratio between the primary and additional frequencies will occur at half-odd integers, i.e.,  $1/2, 3/2, 5/2, \dots$ . However, the peak strength will diminish for the higher order term as it is determined by the higher order Bessel function. Studying such frequency dependence of the AC Josephson current will give an indication of the fractionalized PDW order.

#### Appendix D: Extracting the envelope

The Josephson current for a PDW state or fractionalized PDW state shows a beat-like structure. Such a beat-like form can be distinguished in experiments establishing an entanglement between the superconducting and the charge orders. To provide a detailed description, it becomes necessary to determine the parameters that control such a current envelope. In this section, we provide the details of the envelope of the Josephson current. We start with Eq.(C2) Using trigonometric identities, we obtain

$$I_J = \frac{\kappa n}{\hbar} \sin \theta_0 + \frac{t_0 \sqrt{nn'}}{\hbar} \sin \left( \theta_0 + \frac{\phi_0 - \theta_0}{2} \right) + \frac{\kappa n}{\hbar} \sin \theta_0 + \frac{t_0 \sqrt{nn'}}{\hbar} \sin \left( \theta_0 - \frac{\phi_0 + \theta_0}{2} \right). \quad (\text{D1})$$

Before adding the sine waves we define,  $(\phi_0 - \theta_0)/2 = \chi_1$  and  $(\phi_0 + \theta_0)/2 = \chi_2$ . Therefore, using  $n \approx n'$ , the expression current becomes,

$$I_J = \frac{n}{\hbar} \left[ \sqrt{\kappa^2 + t_0^2 + 2\kappa t_0 \cos \chi_1} \sin(\theta_0 + \xi_1) + \sqrt{\kappa^2 + t_0^2 + 2\kappa t_0 \cos \chi_2} \sin(\theta_0 - \xi_2) \right]. \quad (\text{D2})$$

Here the phase angles  $\xi_i$  are given by

$$\xi_i = \sin^{-1} \left( \frac{t_0 \sin \chi_i}{\sqrt{\kappa^2 + t_0^2 + 2\kappa t_0 \cos \chi_i}} \right), \quad (\text{D3})$$

where  $i = 1, 2$ . Since,  $t_0$  is the small parameter in our calculations, the phase shifts can be assumed to be small, such that  $\xi_i = 0$ . Therefore the current becomes

$$I_J = \frac{n}{\hbar} \sum_{i=1}^2 \left[ \sqrt{\kappa^2 + t_0^2 + 2\kappa t_0 \cos \chi_i} \right] \sin(\theta_0). \quad (\text{D4})$$

Here the amplitude of the envelope is controlled by two phases. The faster oscillation is governed by  $\chi_2 = (\phi_0 + \theta_0)/2$  and the slower one by  $\chi_1 = (\phi_0 - \theta_0)/2$ .

#### Appendix E: Josephson current with dephasing parameter

##### 1. Electric field parallel to $Q_0$

In this appendix, we discuss the difficulty of detecting the Josephson current's oscillation after a finite time  $t$  the electric field is switched on. For times  $t \gg r_0$ , the transient current and also  $\theta'_0 \rightarrow 0$ . As a consequence, at a finite time, the Josephson current for fractionalized PDW is given by

$$I_J(t) = \frac{2\kappa n}{\hbar} \sin(\alpha t + C_1) + \frac{2(t_0 + t_1)\sqrt{nn'}}{\hbar} \sin \frac{\alpha t + C_1}{2} \times \cos \frac{\gamma}{2} + \frac{2(t_0 - t_1)}{\pi \hbar} \sqrt{\frac{n'}{n}} \sin \frac{\gamma}{2} \sin \frac{\alpha t + C_1}{2}, \quad (\text{E1})$$

where we have redefined  $\alpha = 2\mu_\Delta/\hbar$ . We can observe that the current becomes independent of the modulation wavevector  $Q_0$ , if we study the current after time  $t > r_0$ , the electric field is turned on.

##### 2. Electric field perpendicular to $Q_0$

No such complications arise when the JJ is set up so that the wavevector is perpendicular to the electric field. In this case, although  $r_0 = 0$  and the transient current cannot survive, yet  $\theta'_0 = Q_0 \delta$ . Here  $\delta$  denotes the phase difference between the CDW wavevector in the two terminals. Consequently, the dependence of the Josephson current on the  $Q_0$  survives in this setup even for finite  $t$ .

<sup>1</sup> M. H. Hamidian et al., *Nature* **532**, 343 (2016). [I](#)

<sup>2</sup> J. E. Hoffman et al., *Science* **295**, 466 (2002).

<sup>3</sup> W. D. Wise et al., *Nat. Phys.* **4**, 696 (2008).

<sup>4</sup> J.-J. Wen et al., *Nature communications* **10**, 1 (2019).

<sup>5</sup> T. Wu et al., *Nature Communications* **6**, 6438 (2015).

<sup>6</sup> J. Q. Lin et al., *Phys. Rev. Lett.* **124**, 207005 (2020). [I](#)

<sup>7</sup> G. Baskaran and P. W. Anderson, *Phys. Rev. B* **37**, 580 (1988). [I](#)

<sup>8</sup> P. A. Lee and N. Nagaosa, *Phys. Rev. B* **46**, 5621 (1992).

<sup>9</sup> K.-Y. Yang, W. Q. Chen, T. M. Rice, M. Sigrist, and F.-C. Zhang, *New Journal of Physics* **11**, 055053 (2009). [I](#)

<sup>10</sup> D. Chakraborty et al., *Phys. Rev. B* **100**, 224511 (2019). [IA](#), [IC](#), [V](#)

<sup>11</sup> M. Grandadam, D. Chakraborty, and C. Pépin, *Journal of Superconductivity and Novel Magnetism* **33**, 2361 (2020).

<sup>12</sup> C. Pépin, D. Chakraborty, M. Grandadam, and S. Sarkar, *Annual Review of Condensed Matter Physics* **11**, 301 (2020).

<sup>13</sup> M. Grandadam, D. Chakraborty, X. Montiel, and C. Pépin, Phys. Rev. B **102**, 121104 (2020). **IA, IC, V**

<sup>14</sup> H. Alloul, T. Ohno, and P. Mendels, Phys. Rev. Lett. **63**, 1700 (1989). **IC**

<sup>15</sup> H. Alloul, P. Mendels, H. Casalta, J. F. Marucco, and J. Arabski, Phys. Rev. Lett. **67**, 3140 (1991).

<sup>16</sup> W. W. Warren et al., Phys. Rev. Lett. **62**, 1193 (1989). **IC**

<sup>17</sup> N. Doiron-Leyraud et al., Nature **447**, 565 (2007). **IC**

<sup>18</sup> S. Blanco-Canosa et al., Phys. Rev. Lett. **110**, 187001 (2013).

<sup>19</sup> S. E. Sebastian et al., Phys. Rev. Lett. **108**, 196403 (2012).

<sup>20</sup> J. Chang et al., Nat. Commun. **7**, 11494 (2016).

<sup>21</sup> T. Wu et al., Nature **477**, 191 (2011). **IC**

<sup>22</sup> S. Gerber et al., Science **350**, 949 (2015). **IC**

<sup>23</sup> J. Chang et al., Nat. Commun. **7** (2016).

<sup>24</sup> T. Machida et al., Nature Communications **7**, 11747 (2016). **IC**

<sup>25</sup> D. H. Torchinsky, F. Mahmood, A. T. Bollinger, I. Božović, and N. Gedik, Nature Materials **12**, 387 (2013). **IC**

<sup>26</sup> L. Nie, G. Tarjus, and S. A. Kivelson, Proc. Natl. Acad. Sci. **111**, 7980 (2014).

<sup>27</sup> L. Nie, L. E. H. Sierens, R. G. Melko, S. Sachdev, and S. A. Kivelson, Phys. Rev. B **92**, 174505 (2015).

<sup>28</sup> A. Banerjee, A. Garg, and A. Ghosal, Phys. Rev. B **98**, 104206 (2018).

<sup>29</sup> G. Campi et al., Nature (London) **525**, 359 (2015). **IC**

<sup>30</sup> S. D. Edkins et al., Science **364**, 976 (2019). **IC, III B**

<sup>31</sup> P. Choubey et al., Proceedings of the National Academy of Sciences **117**, 14805 (2020).

<sup>32</sup> Z. Du et al., Nature **580**, 65 (2020). **V**

<sup>33</sup> Z. Shi, P. Baity, J. Terzic, T. Sasagawa, and D. Popović, Nature communications **11**, 1 (2020). **IC, V**

<sup>34</sup> A. Barone and G. Paterno, *Physics and applications of the Josephson effect*, Wiley, 1982. **II, III A, B**

<sup>35</sup> P. Lee and T. Rice, Physical Review B **19**, 3970 (1979). **II**

<sup>36</sup> G. Grüner, Rev. Mod. Phys. **60**, 1129 (1988). **III A, B**

<sup>37</sup> B. Loret et al., Nature Physics **15**, 771 (2019). **V**

<sup>38</sup> S. Sachdev and R. La Placa, Phys. Rev. Lett. **111**, 027202 (2013). **V**

<sup>39</sup> A. Allais, D. Chowdhury, and S. Sachdev, Nature communications **5**, 1 (2014).

<sup>40</sup> A. Allais, J. Bauer, and S. Sachdev, Phys. Rev. B **90**, 155114 (2014).

<sup>41</sup> M. R. Norman, M. Randeria, H. Ding, and J. C. Campuzano, Phys. Rev. B **57**, R11093 (1998).

<sup>42</sup> C.-C. Chien, Y. He, Q. Chen, and K. Levin, Phys. Rev. B **79**, 214527 (2009). **V**

<sup>43</sup> P. Lozano, G. Gu, J. Tranquada, and Q. Li, Physical Review B **103**, L020502 (2021). **V**

<sup>44</sup> M. S. Scheurer et al., Proceedings of the National Academy of Sciences **115**, E3665 (2018). **V**

<sup>45</sup> S. Sachdev, H. D. Scammell, M. S. Scheurer, and G. Tarnopolsky, Phys. Rev. B **99**, 054516 (2019).

<sup>46</sup> Z. Nussinov and J. Zaanen, Stripe fractionalization i: The generation of king local symmetry, in *Journal de Physique IV (Proceedings)*, volume 12, pages 245–250, EDP sciences, 2002.

<sup>47</sup> J. Zaanen and Z. Nussinov, physica status solidi (b) **236**, 332 (2003).

<sup>48</sup> P. A. Lee, N. Nagaosa, T.-K. Ng, and X.-G. Wen, Phys. Rev. B **57**, 6003 (1998).

<sup>49</sup> Z. Dai, Y.-H. Zhang, T. Senthil, and P. A. Lee, Phys. Rev. B **97**, 174511 (2018). **V**